Computerized Design and Analysis of Face-Milled, Uniform Tooth Height Spiral Bevel Gear Drives

Faydor L. Litvin and Anngwo Wang
University of Illinois at Chicago
Chicago, Illinois

R.F. Handschuh
Vehicle Propulsion Directorate
U.S. Army Research Laboratory
Lewis Research Center
Cleveland, Ohio

19961129 016

DTIC QUALITY INSPECTED

National Aeronautics and
Space Administration

U.S. ARMY

RESEARCH LABORATORY

COMPUTERIZED DESIGN AND ANALYSIS OF FACE-MILLED, UNIFORM TOOTH HEIGHT SPIRAL BEVEL GEAR DRIVES

Faydor L. Litvin and Anngwo Wang
Department of Mechanical Engineering
University of Illinois at Chicago
Chicago, Illinois

R. F. Handschuh
Army Research Laboratory
NASA Lewis Research Center
Cleveland, Ohio

ABSTRACT

Face-milled spiral bevel gears with uniform tooth height are considered. An approach is proposed for the design of low-noise and localized bearing contact of such gears. The approach is based on the mismatch of contacting surfaces and permits two types of bearing contact either directed longitudinally or across the surface to be obtained. A Tooth Contact Analysis (TCA) computer program was developed. This analysis was used to determine the influence of misalignment on meshing and contact of the spiral bevel gears. A numerical example that illustrates the developed theory is provided.

1 INTRODUCTION

Two models for spiral bevel gears with uniform tooth height were proposed by Litvin et al [6]. The generation of tooth surfaces of such gears is based on application: (i) of two cones that are in tangency along their common generatrix (model 1), and (ii) a cone and a surface of revolution that are in tangency along a common circle (model 2).The pinion and the gear are face-milled by head-cutters whose blades by rotation form the generating surfaces.

The generating surfaces provide conjugate pinion-gear tooth surfaces with a localized bearing contact that is formed by a set of instantaneous contact ellipses. The path of contact is directed across the surfaces in model 1 (fig. 1), and in the longitudinal direction in model 2 (fig. 2). The transmission errors are zero but only for aligned gear drives.

It is well known that misalignment of a gear drive causes the shift of the bearing contact and transmission errors. The transmission errors are one of the main sources of vibration. Therefore, the direct application of the models discussed above for generating surfaces is undesirable.

It was discovered that misalignment of a gear drive causes an almost linear but discontinuous transmission function. However, such functions can be absorbed by a predesigned parabolic function of transmission errors. The interaction of the parabolic function and a linear function results a parabolic function with the same parabola coefficient [9]. Based on this consideration, it becomes necessary to modify the process for generation discussed above to obtain a predesigned parabolic function of transmission errors. It was proposed in work [10] to obtain the desired parabolic function of transmission errors by executing proper nonlinear relations between the motions of the cradle and the gear (or the pinion) being generated. This approach requires the application of the CNC machines.

The purpose of this paper is to propose modifications of generating surfaces that will obtain: (i)a localized bearing contact that may be directed in the longitudinal direction or across the surface, and (ii)a predesigned parabolic function. These goals that will be proven later are obtained by the proper mismatch of the ideal generating surfaces shown in figs.1 and 2. The mismatch of surfaces is achieved by application of modified generating surfaces shown in fig. 3. The modified generating surfaces are in point contact instead of tangency along a line that the ideal generating surfaces have. The desired parabolic function of transmission errors, the orientation of the path of contact, and the magnitude of the major axis of the contact ellipses are obtained by the proper determination of the curvature and the mean radius of the surface of revolution of the generating tool.

The meshing and contact of the tooth surfaces was simulated by the TCA computer program developed by the authors. Numerical examples for the illustration of the proposed approach are considered.

2 METHOD FOR GENERATION OF CONJUGATE PINION-GEAR TOOTH SURFACES

Gear Generation:

The head-cutter for gear generation is provided with inner and outer straight-line blade (fig. 4), that form two cones while the blades are rotated about the Z_{t_2}-axis of the head cutter. These cones will generate the convex and concave sides of the space of the gear, respectively.

We apply coordinate systems S_{c_2}, S_2, S_m that are rigidly connected to the cradle of the generating machine, the gear and the cutting machine, respectively (figs. 5 and 6). The cradle with coordinate system S_{c_2} performs rotation about the Z_m-axis, and ψ_{c_2} is the current angle of rotation of the cradle (We take $i = 2$ in the designations of fig. 5). Coordinate system S_{t_2} is rigidly connected to the gear head-cutter that is mounted on the cradle. The installment of the head-cutter is determined with angle q_2 and $S_{r_2} = |\overline{O_{c_2}O_{t_2}}|$ (fig. 5(b)). The gear in the process for generation performs rotation about the Z_b-axis of the auxiliary fixed coordinate system S_b that is rigidly connected to the S_m coordinate system (fig. 6). The installment of S_b with respect to S_m is determined with angle γ_2, where γ_2 is the angle of the gear pitch cone. The current angle of gear rotation is ψ_2 (fig. 6). Angles ψ_{c_2} and ψ_2 are related as

$$\frac{\psi_{c_2}}{\psi_2} = \frac{\omega_{c_2}}{\omega_2} = \sin\gamma_2 \qquad (1)$$

The observation of this equation guaranties that the X_m-axis is the instantaneous axis of rotation of the gear in its relative motion with respect to the cradle.

Pinion Generation:

The head-cutters for pinion generation are provided with separate blades that will generate the convex and concave sides of the space of the pinion, respectively (fig. 7). The pinion generating tool is installed on the cradle similarly to the installment of the gear generating cone (We take $i = 1$ in the designations of fig. 5). An auxiliary fixed coordinate system S_a is rigidly connected to the S_m coordinate system (fig. 8). The installment of S_a with respect to S_m is determined with angle γ_1 of the pinion pitch cone. An imaginary process for the pinion generation for the purpose of simplification of the TCA program is considered. The installment of coordinate system S_a with respect to S_m is determined in the real process of cutting by the angle γ_1 that is measured clockwise, opposite to the direction shown in fig. 8. The pinion performs rotation about the Z_a-axis and ψ_1 is the current angle of rotation. The angles of rotation of the pinion and the cradle are related as

$$\frac{\psi_{c_1}}{\psi_1} = \frac{\omega_{c_1}}{\omega_1} = \sin\gamma_1 \qquad (2)$$

Axis X_m in accordance to equation (2) is the instantaneous axis of rotation of the pinion in its relative motion with respect to the cradle.

3 DERIVATION OF GEAR TOOTH SURFACE

We consider that the gear head-cutter surface is represented in S_{t_2} by vector function $\mathbf{r}_{t_2}(s_g, \theta_g)$, where s_g and θ_g are the surface parameters. A family of tool surfaces is generated in gear coordinate system S_2 while the cradle and the mounted tool and the gear perform the rotational motions that are shown in figs. 5 and 6. The family of surfaces is represented in S_2 by the matrix equation

$$
\begin{aligned}
\mathbf{r}_2(s_g, \theta_g, \psi_2) &= \mathbf{M}_{2b}(\psi_2)\mathbf{M}_{bm}\mathbf{M}_{mc_2}(\psi_{c_2})\mathbf{M}_{c_2t_2}\mathbf{r}_{t_2}(s_g, \theta_g) \\
&= \mathbf{M}_{2t_2}\mathbf{r}_{t_2}(s_g, \theta_g)
\end{aligned}
\qquad (3)
$$

The product of matrices $\mathbf{M}_{2t_2}$ is based on the coordinate transformations from S_{t_2} to S_2 (figs. 5 and 6). The derivation of vector function $\mathbf{r}_{t_2}(s_g, \theta_g)$ is represented in Appendix 1.

The envelope to the family of surfaces $\mathbf{r}_2(s_g, \theta_g, \psi_2)$ is determined with equation (3) and the equation of meshing is [9]

$$\mathbf{N}_{c_2} \cdot \mathbf{v}_{c_2}^{(c_2 2)} = f_2(s_g, \theta_g, \psi_2) = 0 \qquad (4)$$

where $\mathbf{N}_{c_2}$ is the normal to the generating surface, and $\mathbf{v}_{c_2}^{(c_2 2)}$ is the relative velocity of the tool with respect to the gear. Vectors in equation (4) are represented in coordinate system S_{c_2}.

An alternative approach for the derivation of the equation of meshing is based on the consideration that the normal to the generating surface at a point of tangency of the contacting surfaces passes through the instantaneous axis of rotation.

Equations (3) and (4) represent the gear tooth surface by three related parameters. Taking into account that these equations are linear with respect to s_g, we may eliminate s_g and represent the gear tooth surface by two independent parameters, θ_g and ψ_2.

4 DERIVATION OF PINION TOOTH SURFACE

The derivations are similar to those that have been described in section 3. The family of generating surfaces is represented by the matrix equation

$$
\begin{aligned}
\mathbf{r}_1(\lambda_p, \theta_p, \psi_1) &= \mathbf{M}_{1a}(\psi_1)\mathbf{M}_{am}\mathbf{M}_{mc_1}(\psi_{c_1})\mathbf{M}_{c_1t_1}\mathbf{r}_{t_1}(\lambda_p, \theta_p) \\
&= \mathbf{M}_{1t_1}\mathbf{r}_{t_1}(\lambda_p, \theta_p)
\end{aligned}
\qquad (5)
$$

Here, $\mathbf{r}_{t_1}(\lambda_p, \theta_p)$ is the vector function that represents the generating surface (Appendix 2), where λ_p and θ_p are the surface parameters.

The equation of meshing is

$$\mathbf{N}_{c_1} \cdot \mathbf{v}_{c_1}^{(c_1 1)} = f_1(\lambda_p, \theta_p, \psi_1) = 0 \qquad (6)$$

Equations (5) and (6) represent the pinion tooth surface by three related parameters. After elimination of parameter λ_p we may represent the pinion tooth surface by two independent parameters, θ_p and ψ_1.

5 LOCAL SYNTHESIS

The ideas of local synthesis are based on the following considerations [9] :

(1) The pinion and gear tooth surfaces are in tangency at the mean contact point M that is in the middle of the contacting surface.

(2) The gear ratio is equal to the theoretical one.

(3) Considering the principal curvatures of the contacting surfaces, we have to provide in the neighborhood of M the following transmission function (fig. 9)

$$\phi_2(\phi_1) = \frac{N_1}{N_2}\phi_1 - \frac{1}{2}m'_{21}\phi_1^2 \qquad (7)$$

where $\frac{1}{2}m'_{21}$ is the parabola parameter of the predesigned parabolic function of transmission errors

$$\Delta\phi_2(\phi_1) = -\frac{1}{2}m'_{21}\phi_1^2 \qquad (8)$$

(4) In addition it is necessary to provide the desired direction of the contact path.

All these goals can be achieved by the proper mismatch of the contacting surfaces of the pinion-gear tooth surfaces. The procedure of the local synthesis is as follows:

Step 1: We consider as given the surface of the head-cutter that generates the gear tooth surface. The head-cutter surface is a cone and is in line contact with the surface of the gear. One of such contact lines passes through the mean point M of tangency of the pinion and the tooth surfaces. Considering the surface of the gear head-cutter being as known, we determine at point M the principal curvatures and directions of the gear head-cutter.

Step 2: Our next goal is to determine at M the principal curvatures k_s and k_q and directions of the gear tooth surface Σ_2. We apply for this purpose the equations that have been proposed in [9] and represent the direct relations between the principal curvatures and directions for two surfaces being in line contact.

Step 3: We consider at this step that gear and pinion tooth surfaces, Σ_2 and Σ_1, are in tangency at M. As a reminder the mismatched gear and pinion tooth surfaces are in point contact at every instant.

Unit vectors e_s and e_q represent the known directions of the principal directions on surface Σ_2. The principal curvatures k_s and k_q on the gear principal directions are known. Our goal is to determine angle σ_{12} that is formed by vectors e_f and e_s (fig. 10) and the principal curvatures k_f and k_h of the pinion tooth surface at point M. Unit vectors e_f and e_h represent the sought-for principal directions on the pinion tooth surface Σ_1.

Step 4: The three unknowns: k_f, k_h and σ_{12} can be determined using the approach developed in [9]. We use for this purpose the following system of three linear equations [9].

$$a_{i1}v_s^{(1)} + a_{i2}v_q^{(1)} = a_{i3} \qquad (i = 1,2,3) \qquad (9)$$

The augmented matrix formed by the coefficients a_{i1}, a_{i2} and a_{i3} is a skew-symmetric one [9]. Here, $v_s^{(1)}$ and $v_q^{(1)}$ are the components of the velocity of the contact point that moves in the process of meshing over the pinion tooth surfaces Σ_1. Coefficients a_{i1}, a_{i2} and a_{i3} are represented in terms of k_s, k_q, k_f, k_h, σ_{12} and the parameters of motion. Coefficient a_{33} contains the derivative

$$m'_{21} = \frac{d}{d\phi_1}(m_{21}(\phi_1)) \qquad (10)$$

where

$$m_{21} = \frac{d\phi_2}{d\phi_1} \qquad (11)$$

Step 5: Equation system (9) represents a system of three linear equations in two unknowns: $v_s^{(1)}$ and $v_q^{(1)}$. Surfaces Σ_1 and Σ_2 are in point contact, the path of contact has a definite direction, and the solution of equation system (9) with respect to $v_s^{(1)}$ and $v_q^{(1)}$ must be unique. Therefore, the rank of the augmented matrix formed by a_{i1}, a_{i2} and a_{i3} is equal to two. This yields that

$$\begin{vmatrix} a_{11} & a_{12} & a_{13} \\ a_{12} & a_{22} & a_{23} \\ a_{13} & a_{23} & a_{33} \end{vmatrix} = F(k_f, k_h, k_s, k_q, \sigma_{12}, m'_{21}) = 0 \qquad (12)$$

The other relation between the coefficients a_{i1}, a_{i2} and a_{i3} may be determined considering that

$$\tan \eta_1 = \frac{v_q^{(1)}}{v_s^{(1)}} \qquad (13)$$

where η_1 is the assigned direction at M of the tangent to the path of contact on the pinion surface Σ_1.

Using the relations between the coefficients of linear equation (9) discussed above, we are able to determine the sought-for pinion principal curvatures k_f, k_h and orientation angle σ_{12}.

Step 6: We consider now that pinion principal curvatures k_f, k_h and angle σ_{12}, and the principal directions e_f and e_h on surface Σ_1 are known. The generating surface of the head-cutter is designed as a surface of revolution (fig. 3). The pinion head-cutter surface and the pinion tooth surface are in line contact at every instant. Using the direct relations between the principal curvatures and directions for two surfaces being in line contact [9], we may determine the principal curvatures of the pinion head-cutter. Then, the desired mismatch of the surfaces of the gear and the pinion will be obtained by the generation of the gear and the pinion by the designed head-cutters.

Step 7: Knowing the principal curvatures and directions of the pinion and gear tooth surfaces, the elastic approach of the surfaces, we may determine the orientation and the axes of the instantaneous contact ellipse [9].

6 TOOTH CONTACT ANALYSIS

The purpose of TCA is to determine the influence of misalignment on the shift of the bearing contact and the transmission errors. This goal is obtained by the simulation of meshing and contact of pinion and gear tooth surfaces of a misaligned gear drive.

We consider that the pinion and gear tooth surfaces are analytically represented in coordinate systems S_1 and S_2 (see sections 3 and 4, respectively). The meshing of pinion and gear tooth surfaces is considered in fixed coordinate system S_h (figs. 11 and 12). Auxiliary fixed coordinate system S_a and S_e are applied to describe the installment of the pinion with respect to S_h (fig. 11). The pinion alignment error ΔA_p is the pinion axial displacement. The misaligned pinion in the process of meshing with the gear performs rotation about Z_e-axis. The current angle of rotation of the pinion is designated by ϕ_1 (fig. 11).

Auxiliary coordinate systems S_b, S_c and S_d are applied to describe the installment of misaligned gear with respect to S_h. The errors of alignment are: the change $\Delta\gamma$ of the shaft angle (fig. 12), the offset ΔE and the gear axial displacement ΔA_g (fig. 13). The misaligned gear performs rotation about the Z_d-axis, and ϕ_2 is the current angle of the gear rotation.

A TCA computer program was developed to simulate the meshing of pinion-gear tooth surfaces of the misaligned gear drive. The development of the TCA program is based on the following considerations:

Step 1. We consider that the pinion and gear tooth surfaces and the surface unit normals are represented in coordinate system S_1 and S_2 by vector functions

$$\mathbf{r}_i(\theta_i, \psi_i) \qquad (i = 1, 2) \qquad (14)$$

$$\mathbf{n}_i(\theta_i, \psi_i) \qquad (i = 1, 2) \qquad (15)$$

where (θ_i, ψ_i) are the surface parameters.

Step 2. We represent now the pinion-gear tooth surfaces and their surface unit normals in coordinate system S_h, and take into account that the surfaces are in continuous tangency. Then we obtain the following equations

$$\mathbf{r}_h^{(1)}(\theta_1, \psi_1, \phi_1) - \mathbf{r}_h^{(2)}(\theta_2, \psi_2, \phi_2) = 0 \qquad (16)$$

$$\mathbf{n}_h^{(1)}(\theta_1, \psi_1, \phi_1) - \mathbf{n}_h^{(2)}(\theta_2, \psi_2, \phi_2) = 0 \qquad (17)$$

Equations (16) and (17) represent the conditions that the contacting surfaces at the point of tangency have a common position vector and a common surface unit normal. Equations (16) and (17) yield a system of five independent scalar equations of the following structure

$$f_i(\theta_1, \psi_1, \phi_1, \theta_2, \psi_2, \phi_2) = 0 \qquad f_i \in C^1 \qquad (i = 1..5) \quad (18)$$

As a reminder vector equation (17) yields only two independent scalar equations and not three, since $|\mathbf{n}_h^{(1)}| = |\mathbf{n}_h^{(2)}| = 1$.

Step 3. System (18) of five nonlinear equations contains six unknowns, but one of the unknowns, say ϕ_1, may be considered as the input parameter. Our goal is the numerical solution of nonlinear equations (18) by functions

$$\{\theta_1(\phi_1), \psi_1(\phi_1), \theta_2(\phi_1), \psi_2(\phi_1), \phi_2(\phi_1)\} \in C^1 \qquad (19)$$

The sought-for numerical solution is an iterative process that requires on each iteration the observation of the following conditions [9][3]:

(i) There is a set of parameters (the first guess)

$$P(\theta_1^{(o)}, \psi_1^{(o)}, \phi_1^{(o)}, \theta_2^{(o)}, \psi_2^{(o)}, \phi_2^{(o)}) \qquad (20)$$

that satisfies the equation system (18).

(ii) The Jacobian taken at P differs from zero. Thus, we have

$$\Delta_5 = \frac{D(f_1, f_2, f_3, f_4, f_5)}{D(\theta_1, \psi_1, \theta_2, \psi_2, \phi_2)} \neq 0 \qquad (21)$$

Then, as it follows from the Theorem of Implicit Function System Existence, equation system (18) can be solved in the neighborhood of P by functions (19).

Using the obtained solution, we can determine the path of contact on the pinion-gear tooth surface, and the transmission errors caused by misalignment. The path of contact on surface Σ_i ($i = 1, 2$) is determined by the expressions

$$\mathbf{r}_i(\theta_i, \psi_i), \quad \theta_i(\phi_1), \quad \psi_i(\phi_1) \qquad (i = 1, 2) \qquad (22)$$

The transmission errors are determined by equation

$$\Delta\phi_2 = \phi_2(\phi_1) - \frac{N_1}{N_2}\phi_1 \qquad (23)$$

The dimensions and orientations of the instantaneous contact ellipse at the contact point may be determined considering that the principal curvatures and directions of the contacting surfaces, and the elastic approach of the surface [9] are known.

7 NUMERICAL EXAMPLE

The blank data is given in Table 1.

The gear head-cutter is a cone (figs. 2, 3 and 4), the cutter radius is designated by R_g (fig. 1), the radial setting of the head-cutter is $|\overline{O_{c_2}O_{t_2}}|$ (fig. 5(b)), and the installment angle is q_2 (fig. 5). The data for the gear head-cutter that generates the gear concave side are represented in Table 2.

The parameters of the pinion head-cutter were determined by application of the method of local synthesis (section 5). The data for the pinion head-cutter that generates the pinion convex side are represented in Table 3. We

4

considered in the numerical examples the meshing of the gear tooth concave side with the pinion tooth convex side. Case 1 corresponds to the orientation of the bearing contact across the surface, case 2 corresponds to the orientation of the bearing contact in the longitudinal direction.

The application of TCA for the simulation of meshing and contact permits the determination of misalignment effects on the transmission errors and the shift of the bearing contact. It has been shown that in the case of application of ideal generating surfaces (without mismatch, figs. 1 and 2) the errors of misalignment cause indeed discontinuous almost linear transmission errors as shown in fig. 14 for shaft angle error $\Delta\gamma$. Similar functions of transmission errors are caused by errors ΔA_p, ΔA_g and ΔE. Table 4 shows the maximal transmission errors caused by misalignment.

The results of TCA for the properly mismatched generating surfaces (see section 5) confirmed that a predesigned parabolic function indeed absorbs the transmission errors caused by misalignment, and the resulting function of transmission is a parabolic one (fig. 15). The absorption of linear function of transmission errors is carried out as well in other cases of misalignment: ΔA_p, ΔA_g and ΔE. The bearing contact of the drive is stabilized, and its shift is permissible (fig. 16). Model 2 of the gear drive (with longitudinal direction of the bearing contact) is preferable due to the lower level of transmission errors caused by misalignment.

8 CONCLUSION

From the study conducted the following general conclusions can be drawn:

(1) An approach has been developed for the synthesis of spiral bevel gears that provides: (i) localized bearing contact, and (ii) low level of transmission errors of a parabolic type. The approach developed permits two possible directions of the bearing contact: across the tooth surface or in the longitudinal direction.

(2) A Tooth Contact Analysis (TCA) computer program for the investigation of the influence of misalignment on the shift of the bearing contact was developed.

(3) The low level of transmission errors, the parabolic type of the function of transmission errors, and the localization of the bearing contact are achieved by the proper mismatch of contacting surfaces.

(4) The influence of the following errors of alignment was investigated: (i) for axial displacement of the pinion, (ii) axial displacement of the gear, (iii) offset, and (iv) change of the shaft angle. These types of misalignment were proven to cause discontinuous almost linear functions of transmission errors, but they are absorbed by the predesigned parabolic function of transmission errors.

The results of this investigation show that a predesigned parabolic function can indeed absorb the linear functions of transmission errors caused by misalignment. The design of gears with a longitudinal bearing contact (in comparison with the bearing contact across the surface) is preferable since a lower level of transmission errors can be obtained.

REFERENCES

[1] Dongarrd, J.J., Bunch, J.R., Moler, C.B., and Steward, G.W. 1979. LINPACK User's Guide, SIAM, Philadelphia

[2] Favard, J. Course of Local Differential Geometry, Gauthier-Villars, Paris (in French, translated into Russian)

[3] Korn, G.A. and Korn, T.M. 1968. Mathematics Handbook for Scientists and Engineers, 2nd ed., McGraw-Hill, NY.

[4] Litvin, F.L. 1960, 1968. Theory of Gearing, 1st ed. (1960), 2nd ed. (1968). Nauka (in Russian)

[5] Litvin, F.L. 1969. Die Beziehungen Zwischen den Krümmungen der Zahnoberflächen bei Räumlichen Verzahnungen. Z. Angew. Math. Mech. 49: 685-690 (in German)

[6] Litvin, F.L. Pahman P. and Goldrich R.N. 1982, Mathematical Models for the Synthesis and Optimization of Spiral Bevel Gear Tooth Surfaces, NASA CR-3553

[7] Litvin, F.L. 1989. Theory of Gearing, NASA Reference Publication 1212

[8] Litvin, F.L. and Zhang, Y. 1991. Local Synthesis and Tooth Contact Analysis of Face-Milled Spiral Bevel Gears. NASA Contractor Report 4342, AVSCOM Technical Report 90-C-028

[9] Litvin, F.L. 1994. Gear Geometry and Applied Theory, Prentice Hall

[10] Litvin, F. L. and Zhao, X. 1996. Computerized Design and Analysis of Face-milled, Uniform Tooth Height, Low-Noise Spiral Bevel Gear Drives, NASA Contractor Report 4704.

[11] More, Jorge J., Garbow, Burton S., and Hilstorm, Kenneth E. 1980. User Guide for MINPACK-1, Argonne National Laboratory, Argonne, IL.

[12] Stadtfeld, H.J. 1993. Handbook of Bevel and Hypoid Gears. Rochester Institute of Technology

[13] Zalgaller, V.A. 1975. Theory of Envelopes, Nauka, Moscow (in Russian)

APPENDIX 1
Equations of Gear Generating Surfaces
The generating cone represented in S_{t_2} is

$$\mathbf{r}_{t_2}(s_g, \theta_g) = \begin{bmatrix} (R_g - s_g \sin \alpha_g) \cos \theta_g \\ (R_g - s_g \sin \alpha_g) \sin \theta_g \\ s_g \cos \alpha_g \end{bmatrix} \quad (24)$$

where s_g and θ_g are the surface coordinates; α_g is the blade angle; R_g is the radius of the head-cutter at mean point. Equations (24) may also represent the convex side of the generating cone considering that α_g is negative.

Coordinate system S_{t_2} is rigidly connected to coordinate system S_{c_2}, and the unit normal to the gear generating surface is represented by the equations

$$\mathbf{n}_{c_2}(\theta_g) = \frac{\mathbf{N}_{c_2}}{|\mathbf{N}_{c_2}|} \ , \quad \mathbf{N}_{c_2} = \frac{\partial \mathbf{r}_{t_2}}{\partial \theta_g} \times \frac{\partial \mathbf{r}_{t_2}}{\partial s_g} \qquad (25)$$

Equations (24) and (25) yield

$$\mathbf{n}_{c_2}(\theta_g) = \begin{bmatrix} \cos\alpha_g \cos\theta_g \\ \cos\alpha_g \sin\theta_g \\ \sin\alpha_g \end{bmatrix} \qquad (26)$$

APPENDIX 2
Equations of Pinion Generating Surfaces

The generating surface of revolution is represented in S_{t_1} as

$$\mathbf{r}_{t_1}(\lambda_p,\theta_p) = \begin{bmatrix} [R_p - R_1(\cos\alpha_p - \cos(\alpha_p + \lambda_p))]\cos\theta_p \\ [R_p - R_1(\cos\alpha_p - \cos(\alpha_p + \lambda_p))]\sin\theta_p \\ -R_1(\sin\alpha_p - \sin(\alpha_p + \lambda_p)) \end{bmatrix} \qquad (27)$$

where λ_p and θ_p are the generating surface coordinates; α_p is the profile angle at M point; R_p is the radius of the head-cutter at mean point; R_1 is the radius of surface of revolution. Equations (27) can also represent the concave side of the generating surface of revolution if we substitute α_p as $180° - \alpha_p$.

Coordinate system S_{t_1} is rigidly connected to coordinate system S_{c_1}, and the unit normal to the pinion generating surface is represented by the equations

$$\mathbf{n}_{c_1}(\lambda_p,\theta_p) = \frac{\mathbf{N}_{c_1}}{|\mathbf{N}_{c_1}|} \ , \quad \mathbf{N}_{c_1} = \frac{\partial \mathbf{r}_{t_1}}{\partial \theta_p} \times \frac{\partial \mathbf{r}_{t_1}}{\partial \lambda_p} \qquad (28)$$

Equations (27) and (28) yield

$$\mathbf{n}_{c_1}(\lambda_p,\theta_p) = \begin{bmatrix} \cos\theta_p \cos(\alpha_p + \lambda_p) \\ \sin\theta_p \cos(\alpha_p + \lambda_p) \\ \sin(\alpha_p + \lambda_p) \end{bmatrix} \qquad (29)$$
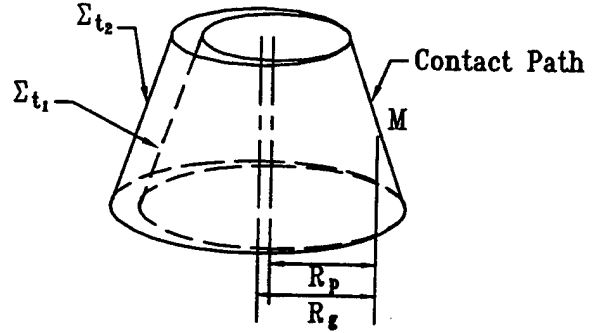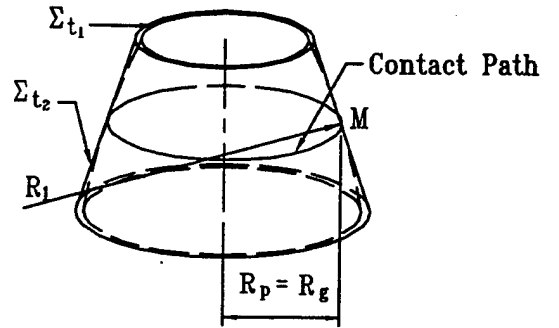

FIGURE 1: Generating cones

FIGURE 2: Generating cone and generating surface of revolution
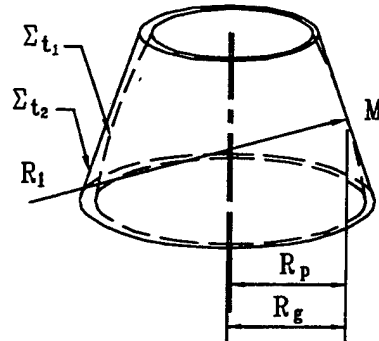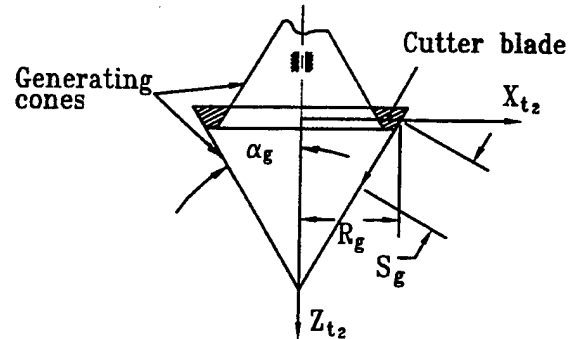

FIGURE 3: Mismatched generating surfaces

FIGURE 4: Cones for gear generation
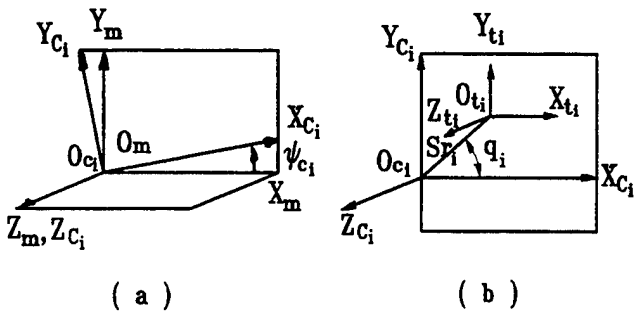
TABLE 1: Blank Data

	Pinion	Gear
N_1, N_2, Number of teeth	11	41
γ, Shaft angle	90°	
Mean spiral angle	35°	35°
Hand of spiral	RH	LH
Whole depth (mm)	10.0	10.0
γ_1, γ_2, Pitch angles	15°1'	74°59'

FIGURE 5: Coordinate systems S_c and S_m

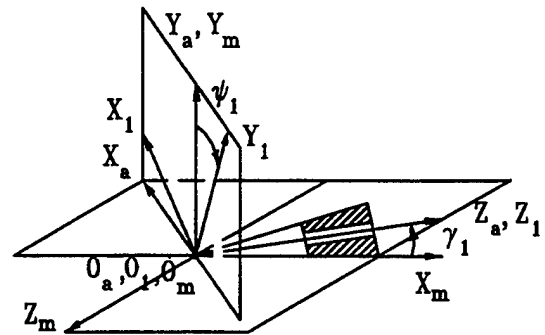FIGURE 8: Coordinate systems S_m, S_a and S_1

FIGURE 6: Coordinate systems S_m, S_b and S_2
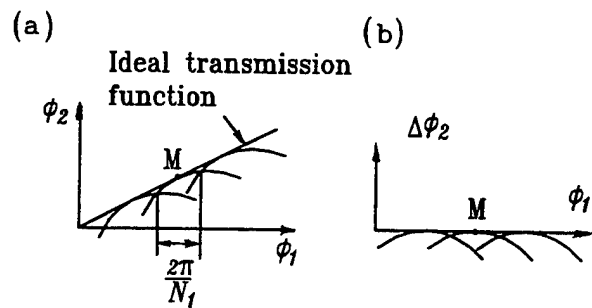

(a)   (b)

FIGURE 9: Transmission function and predesigned parabolic function of transmission errors, ϕ_1-pinion rotation angle; ϕ_2-gear rotation angle; $\Delta\phi_2$-transmission error
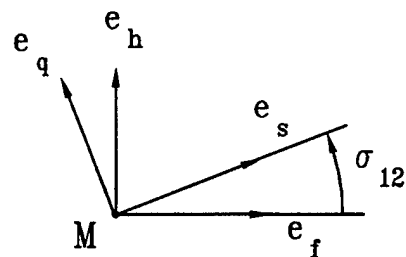

FIGURE 10: Unit vectors of principal directions of surfaces Σ_2 and Σ_1

FIGURE 7: (a)Convex (inside blade) and (b)concave (outside blade) sides of the generating blades and generating surfaces of revolution

TABLE 2: Parameters and Installment of Gear Head-Cutter on gear concave side

α_g, Blade angle	$20°$
R_g, Cutter radius at mean point (mm)	78.52
S_{r2}, Radial setting (mm)	70.53
q_2, Installment angle	$-62°14'$

7

TABLE 3: Parameters and Installment of the Pinion Head-Cutter on pinion convex side

	Case 1	Case 2
α_p	20°	20°
q_1	−61°51′	−51°24′
INPUT		
η_1	171°	92°
m'_{21}	-1.3e-3	-1.2e-3
$\Delta\phi_2$	-10.94	-10.09
OUTPUT		
M	(79.88, 0.39, 0.17)	(77.83, 1.64, 0.72)
$R_p(mm)$	78.0	64.7
$R_1(mm)$	235.0	765.0
2a (mm)	12.54	4.5

TABLE 4: Maximum Transmission Errors for Generating Surfaces with Mismatch

	$\Delta\phi_2$ in arc sec.	
	Case 1	Case 2
$\Delta A_p = 0.1mm$	8.8	16.2
$\Delta A_g = 0.1mm$	11.5	12.5
$\Delta E = 0.1mm$	11	15
$\Delta\gamma = 3'$	10.7	13.5

(a)   (b)
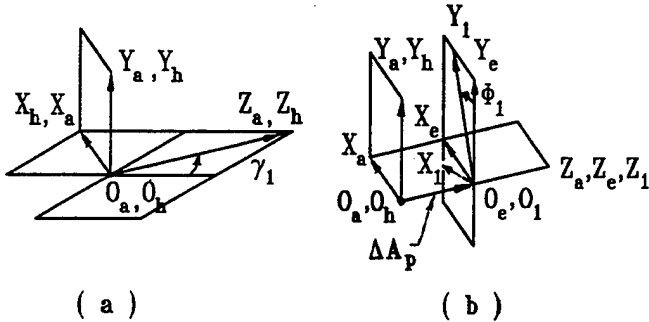
FIGURE 11: Simulation of pinion misalignment ΔA_p

(a)   (b)
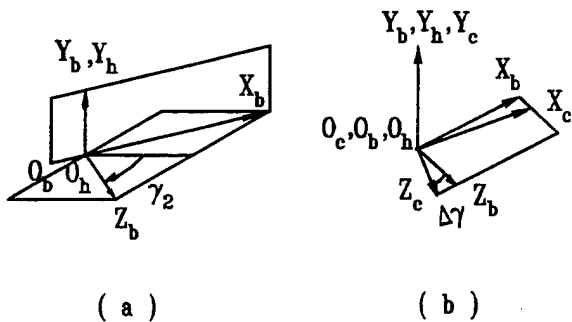
FIGURE 12: Simulation of gear misalignment $\Delta\gamma$
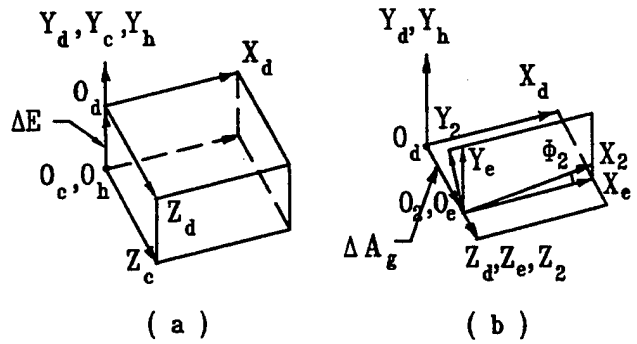

(a)   (b)

FIGURE 13: Simulation of gear misalignment ΔE and ΔA_g
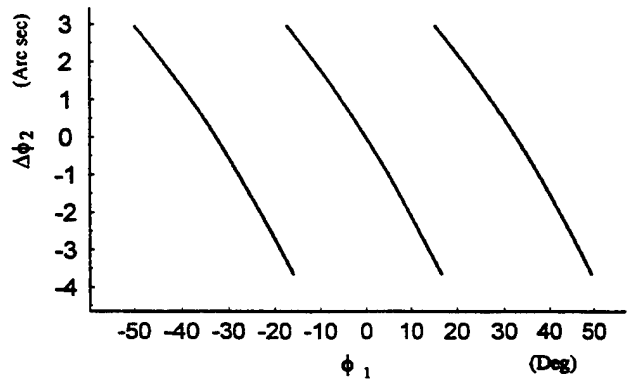

FIGURE 14: Transmission errors for a misaligned gear drive with ideal surfaces: $\Delta\gamma = 3$ arc min.
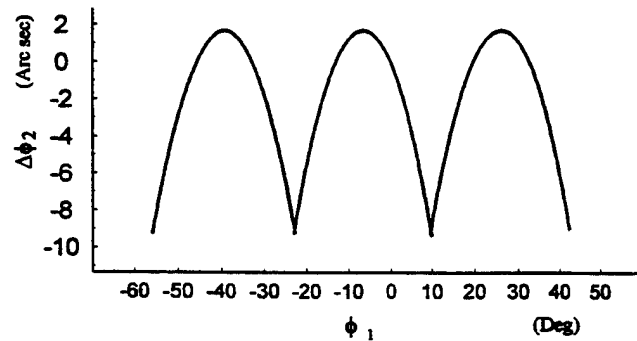

FIGURE 15: Transmission errors for a misaligned gear drive with mismatched gear tooth surfaces: $\Delta\gamma = 3$ arc min.
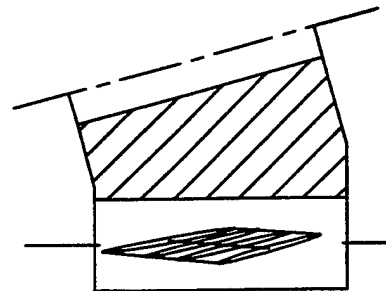

FIGURE 16: Longitudinal bearing contact for a misaligned gear drive ($\Delta\gamma = 3$ arc min.)

8

REPORT DOCUMENTATION PAGE

Public reporting burden for this collection of information is estimated to average 1 hour per response, including the time for reviewing instructions, searching existing data sources, gathering and maintaining the data needed, and completing and reviewing the collection of information. Send comments regarding this burden estimate or any other aspect of this collection of information, including suggestions for reducing this burden, to Washington Headquarters Services, Directorate for Information Operations and Reports, 1215 Jefferson Davis Highway, Suite 1204, Arlington, VA 22202-4302, and to the Office of Management and Budget, Paperwork Reduction Project (0704-0188), Washington, DC 20503.

1. AGENCY USE ONLY (Leave blank)	2. REPORT DATE	3. REPORT TYPE AND DATES COVERED
	October 1996	Technical Memorandum

4. TITLE AND SUBTITLE

Computerized Design and Analysis of Face-Milled, Uniform Tooth Height Spiral Bevel Gear Drives

5. FUNDING NUMBERS

WU–505–62–36
1L162211A47A

6. AUTHOR(S)

Faydor L. Litvin, Anngwo Wang, and R.F. Handschuh

7. PERFORMING ORGANIZATION NAME(S) AND ADDRESS(ES)

NASA Lewis Research Center
Cleveland, Ohio 44135–3191
and
Vehicle Propulsion Directorate
U.S. Army Research Laboratory
Cleveland, Ohio 44135–3191

8. PERFORMING ORGANIZATION REPORT NUMBER

E–10499

9. SPONSORING/MONITORING AGENCY NAME(S) AND ADDRESS(ES)

National Aeronautics and Space Administration
Washington, D.C. 20546–0001
and
U.S. Army Research Laboratory
Adelphi, Maryland 20783–1145

10. SPONSORING/MONITORING AGENCY REPORT NUMBER

NASA TM–107348
ARL–TR–1251

11. SUPPLEMENTARY NOTES

12a. DISTRIBUTION/AVAILABILITY STATEMENT

Unclassified - Unlimited
Subject Category 37

This publication is available from the NASA Center for AeroSpace Information, (301) 621–0390.

12b. DISTRIBUTION CODE

13. ABSTRACT (Maximum 200 words)

Face-milled spiral bevel gears with uniform tooth height are considered. An approach is proposed for the design of low-noise and localized bearing contact of such gears. The approach is based on the mismatch of contacting surfaces and permits two types of bearing contact either directed longitudinally or across the surface to be obtained. A Tooth Contact Analysis (TCA) computer program was developed. This analysis was used to determine the influence of misalignment on meshing and contact of the spiral bevel gears. A numerical example that illustrates the developed theory is provided.

14. SUBJECT TERMS

Gears; Transmissions; Spiral bevel gears

15. NUMBER OF PAGES

10

16. PRICE CODE

A02

17. SECURITY CLASSIFICATION OF REPORT	18. SECURITY CLASSIFICATION OF THIS PAGE	19. SECURITY CLASSIFICATION OF ABSTRACT	20. LIMITATION OF ABSTRACT
Unclassified	Unclassified	Unclassified	

NSN 7540-01-280-5500

Standard Form 298 (Rev. 2-89)
Prescribed by ANSI Std. Z39-18
298-102